**International Journal of Environmental Monitoring and Analysis**
2015; 3(2-1): 1-6
Published online October 28, 2014 (http://www.sciencepublishinggroup.com/j/ijema)
doi: 10.11648/j.ijema.2015030201.11
ISSN: 2328-7659 (Print); ISSN: 2328-7667 (Online)

# Analyzing TENORM in hydraulic fracturing wastes

**Leong Ying**

Thermo Fisher Scientific, Hoboken, USA

**Email address:**
leong.ying@thermofisher.com, klystar@gmail.com

**To cite this article:**
Leong Ying. Analyzing TENORM in Hydraulic Fracturing Wastes. *International Journal of Environmental Monitoring and Analysis.* Special Issue: Clean Methods and Technologies for Hydraulic Fracturing. Vol. 3, No. 2-1, 2015, pp. 1-6. doi: 10.11648/j.ijema.2015030201.11

**Abstract:** Hydraulic fracturing, commonly referred to as fracking, is a method used to extract oil and natural gas from shale and coalbed deposits by high-pressure injection of a cocktail mix of chemicals, sand and water. However, absorbed in the returning produced wastewaters along with the desired hydrocarbons are Naturally Occurring Radioactive Material (NORM). Through the various refinement and waste treatment processes these activities can further concentrate the radiological contents into Technologically Enhanced NORM (TENORM). A technique has been developed to perform rapid screening of the radioactivity based on gamma spectroscopy using a scintillation detector with advanced algorithmic processing of the data.

**Keywords:** Hydraulic Fracturing, TENORM, Gamma Spectroscopy

## 1. Introduction

Hydraulic fracturing is a drilled well stimulation process to enhance the exploration of underground resources of oil and natural gas. To maximize the extraction field, wells are typically drilled vertically from a central production pad and then oriented horizontally with both directions extending to several thousands of feet. One of the earliest reported commercial applications was performed in 1947 to stimulate flow of natural gas from the Hugoton field in Kansas. Modern hydraulic fracturing methods have been applied to shale oil and natural gas, and to coalbed methane (CBM) productions [1]. The economic impact of these unconventional gas productions on US energy supplies have been dramatic [2]. Figure 1 is taken from US Energy Information Administration (EIA) productivity report showing the annual productions from new wells drilled at the seven main US shale gas producing basins.

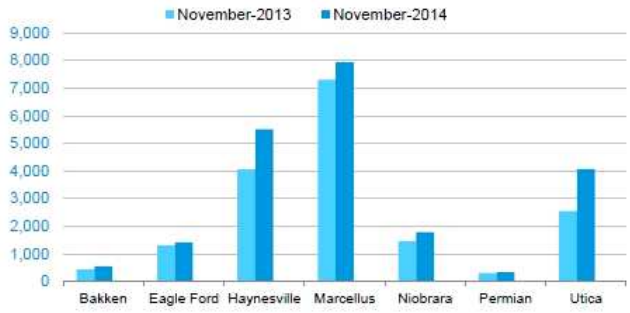


***Figure 1.*** *New well gas productions in thousand cubic feet per day*

Shale gas development has issues related to contamination risks for air, land and water. Contaminants can be from the released methane [3], frac fluids returning in the flowback wastewaters [4] and NORM radioactivity extracted from the drill cuttings and underground processes [5]. Induced earthquakes have also been reported to be associated with hydraulic fracturing [6]. Only by appropriate monitoring and analysis of these risk factors can government regulators set operational rules and processing guidelines to ensure the industry practices do not have adverse environmental and health repercussions.

## 2. Well Stimulation

### *2.1. Hydraulic Fracturing Fluids*

In a report compiled for the US Committee on Energy and Commerce [7], 14 oil and gas companies stated between the periods 2005 to 2009, they used more than 2,500 hydraulic fracturing products containing 750 chemicals and other components. Excluding water added at the well sites, these companies used 780 million gallons of these products over this defined time frame. In this same report, 29 chemicals used in 650 different hydraulic fracturing products were identified as either potential carcinogens or regulated under Safe Drinking Water Act or Clean Air Act.

The injected fluids used by well operators can vary, but typically consists of approximately 90% water, 9% sand and 1% chemicals. There have been trials of non-water fracturing

fluids based on liquefied petroleum gas (LPG) and propane.

This viscous gel mixture carries the sand in suspension and deposits these hard grain proppants into the fractured cavities keeping them porous to allow the released hydrocarbons to flow freely back to the surface. Each of the chemical additives has assigned purposes and will differ in composition depending on the properties and depth of the wells. Table 1 lists the most common categories of chemical additives and their functions.

***Table 1.*** *Common hydraulic fracturing chemical additives*

| Category | Functions |
|---|---|
| Biocides | Prevents bacterial and microorganisms growth |
| Buffers | Acidity control |
| Breakers | Reduce viscosity |
| Corrosion inhibitors | Protect casing and equipment from corrosion |
| Cross-link agents | Support gel formation |
| Friction reducers | Promotes laminar flow |
| Gelling agents | Support proppant carriage |
| Scale inhibitors | Protect casing and equipment from scaling |
| Surfactants | Emulsification |

### *2.2. Water Cycle*

US Environmental Protection Agency (EPA) has produced a comprehensive report study on the potential impacts of hydraulic fracturing on drinking water resources [8].

#### *2.2.1. Acquisition*

Estimates of water requirements range from 65 thousand gallons for each average CBM wells up to 13 million gallons for shale gas production. In comparison, approximately 10 million gallons of water is consumed daily by a general population of 100,000. The main sources of water are typically from ground water, surface water, or recycled treated wastewaters. The availability of local reservoirs and economics of transportation and storage will determine the sourcing of water.

#### *2.2.2. Mixing*

Water is mixed with the chemicals and sand at the drill sites to produce the hydraulic fracturing fluids which serves to create the pressure for propagating fractures in the rocks and to carry the proppant into the opened fractures. The chemicals and sand are transported to the wells by vehicles and typically mixed with the stored water inside mobile slurry blenders and pumping stations. Fracturing equipments are generally rated for operations up to pressures of 15,000psi and injection rates of $10ft^3/s$.

#### *2.2.3. Injection*

Hydraulic fracturing fluids are pumped into wells at sufficient pressure to fracture the oil or gas containing rock strata. A reinforced casing surrounds the wellbore with perforations at the desired fracturing locations. These fractures generally spread out in an orientation perpendicular to the wellbore.

Gas producing rock formations are intentionally fractured at depths that are much deeper than any possible underground water resources. Hence it is important that well casing passing through the upper layers must maintain its integrity during the high-pressure injection to avoid contamination of the surrounding water stratum by seepage of the fracturing fluids.

Fracture monitoring is performed by measuring the pressure and rate during the growth of a hydraulic fracture. On occasions radioactive tracers such as Sc46, Ag110, Tc99 or I131 are used to determine injection profiles and flow rates [9].

#### *2.2.4. Wastewaters*

Direction of fluid flow reverses when the injection pressure is reduced; leading first to the recovery of flowback wastewater returning to the surface, which may contain some of the injected chemicals and compounds naturally occurring in the producing formation including radiological NORM. Produced wastewater is when the returned fluids contain the desired hydrocarbons. These hydraulic fracturing wastewaters are typically stored onsite in artificial ponds or storage tanks.

#### *2.2.5. Treatment and Disposal*

The fraction of hydraulic fracturing fluids returned with the wastewaters varies by geological formation and range from 10% to 70%. The wastewater can be disposed into deep underground injection control (UIC) wells or treated followed by discharge into a water reservoir or reused.

### *2.3. Monitoring and Analysis*

Chemical sampling of hydraulic fracturing fluids and wastewaters can be performed by various laboratory instruments such as by ion chromatography or mass spectrometry [10]. Laboratory analysis of radiological contaminants includes testing methods by indirect radiochemical or direct gamma spectroscopy measurements [11].

Laboratory tests are typically complicated and time consuming, without the ability to conduct real-time field inspections and analysis. These factors can adversely impact productivity and on effective environmental monitoring. For example, a traditional laboratory testing methodology for quantifying the activity concentration of the radioisotope Ra226 requires a 21-days in-growth period of the progeny daughter decay isotope Rn222 (EPA Method 903.1).

## 3. Gamma Spectrometer

### *3.1. Mobile Field Analyzer*

The field applications of a mobile shielded sodium iodide (NaI) scintillation gamma spectrometer used to perform radiological survey of Utica and Marcellus shale was described by Ying [12]. The TENORM radionuclides identified were the radium isotopes Ra226 and Ra228. Radium isotopes are public health concerns because of their solubility in water, which increase their potential for leaching contaminations in flowback and produced wastewaters during the hydraulic fracturing processes. Current industrial recycling procedures applied to the wastewaters can further accumulate these radionuclides in the subsequent solid wastes.

Disposal in landfill sites of these concentrated radium isotopes can potentially have an adverse long-term environmental impact due to emanation of gaseous highly-ionizing radon isotopes as part of the natural decay chains. Hence it is critical for proper environmental monitoring of the radiological impact of these industrial processes to develop an instrument and methodology that can provide accurate and rapid screening of hydraulic fracturing waste products through its complete life cycle from drill sites to midstream waste treatment plants to downstream landfill and water resource recovery facilities.

EPA sets guideline levels of activity concentrations for Ra226. For drinking water the recommended maximum level is 5pCi/L and for solid wastes is 5pCi/g that are regulated respectively under the Clean Water Act (CWA) and Title 40 Code of Federal Regulations (CFR) Part 192.

Figure 2 shows the mobile experimental setup, consisting of a 2in x 2in NaI detector as part of Thermo's RIIDEye handheld isotope identifier integrated into a 0.5in thick lead shield lined with 1mm of pure tin and copper. Samples are collected inside 0.5L Marinelli beakers and top-loaded through the shield's sliding lid. The instruments are factory-calibrated with Co57 (122keV), Cs137 (662keV) and Co60 (1173keV and 1332keV) radioactive sources. An integrated K40 (1460keV) NORM source allows the units to self auto-calibrate during each startup and compensates for thermal instabilities.

***Figure 2.*** *Mobile gamma spectroscopic analyzer*

### *3.2. Natural Decay Chains*

Radium isotopes Ra226 (1,600 years half-life) and Ra228 (5.8 years half-life) are produced in the natural decay series of U238 and Th232 respectively. Figure 3 and 4 show portions of the decay sequence for both radionuclides. Secular equilibrium is achieved when all the radioisotopes in the decay chain are trapped in a closed system for a period that allows all the progeny daughter isotopes to decay into a state of equilibrium. With NORM that has been brought up to the surface and processed into TENORM, then the difference in elemental solubility and escaping radon gas in an opened system will create a non-equilibrium condition. To quantify the activities of specific isotopes, a direct measurement of the decay energies must be performed such as the detection of the 186keV gamma-ray emitted by Ra226, or the parent and daughter isotopes are sealed in a closed system to allow equilibrium to be re-established so that quantification of a daughter product leads to the same measured activity for the parent isotope of interest.

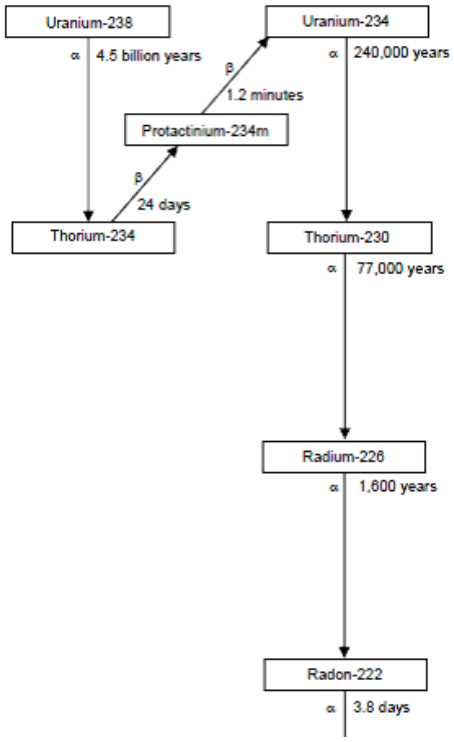


***Figure 3.*** *Ra226 as part of U238 decay chain*

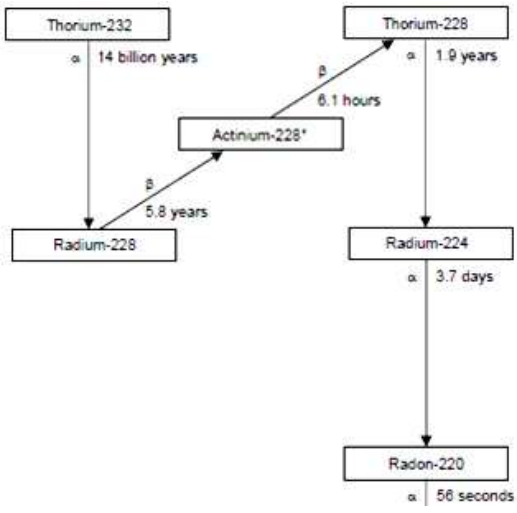


***Figure 4.*** *Ra228 as part of Th232 decay chain*

### *3.3. Detection Efficiencies*

The absolute counting efficiency ($\varepsilon_A$) of a detector is defined as the total number of photons counted ($N_C$) out of the total number of photons ($N_T$) emitted by the sample. It is a function of the absorption cross-section and active thickness

of the detector crystal (intrinsic efficiency $\varepsilon_I$) and the source to detector geometry (geometric efficiency $\varepsilon_G$) which can also be referred to as the geometric solid angle factor [13].

$$\varepsilon_A = \varepsilon_I . \varepsilon_G \quad (1)$$

$$\varepsilon_A = \frac{N_C}{N_T} \quad (2)$$

The total photons emitted by a source sample are a direct function of the radioactivity (r) of the source and sampling time (s).

$$N_T = r.s \quad (3)$$

Detector efficiencies are determined by calibrating the detector systems with known standard sources. Because radioactive sources have decay half-lives ($\tau_{1/2}$), the source activity at any given time ($r_t$) must be corrected for the age (t) of the source since its defining standard's calibration (t=0).

$$r_t = r_0 0.5^{t/\tau_{1/2}} \quad (4)$$

Table 2 lists the parameters for a known Ra226 calibrated source housed in homogenous matrix suspension inside a sealed 0.5L Marinelli beaker. The time of original defining calibration (t=0) of this standard source is certified for traceability to US National Institute of Standards and Technology (NIST). Figure 5 is the energy spectrum taken of the Ra226 standard source using the analyzer instrument over a sampling time of 30 minutes.

***Table 2.*** *NIST-traceable Ra226 standard source*

| Parameters | Ra226 |
|---|---|
| Half-life ($\tau_{1/2}$) | 1600 years |
| Calibration date (t=0) | 19th November 2013 |
| Mass of master source | 0.46117g |
| Mass of matrix (m) | 810.16g |
| Source radioactivity (r) | 195.32Bq (5.28nCi) |
| Uncertainty | ±5% |

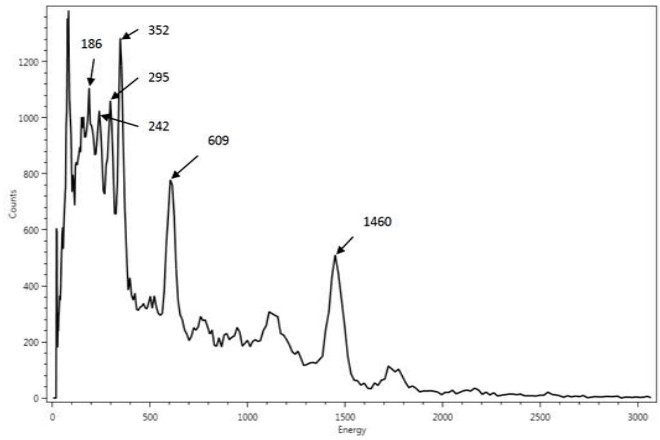


***Figure 5.*** *Ra226 efficiency calibration spectrum*

Table 3 and Figure 6 are the corresponding parameters and calibrated spectrum for the known Ra228 standard source.

***Table 3.*** *NIST-traceable Ra228 standard source*

| Parameters | Ra228 |
|---|---|
| Half-life ($\tau_{1/2}$) | 5.75 years |
| Calibration date (t=0) | 19th November 2013 |
| Mass of master source | 0.10275g |
| Mass of matrix (m) | 813.39g |
| Source radioactivity (r) | 197.29Bq (5.33nCi) |
| Uncertainty | ±5% |

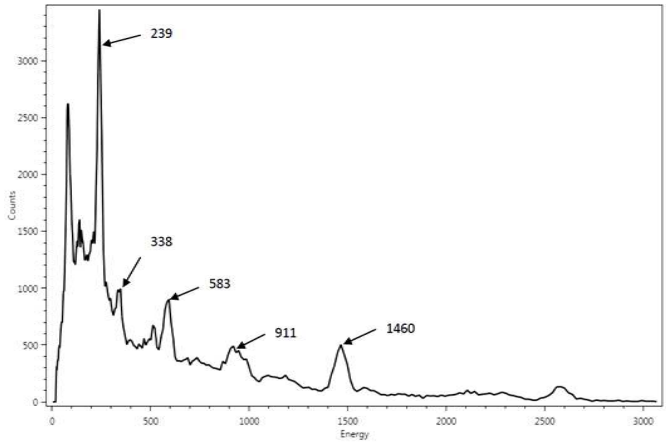


***Figure 6.*** *Ra228 efficiency calibration spectrum*

The energy peaks observed in the two efficiency calibration spectra at 1460keV belongs to the K40 NORM incorporated into the RIIDEye unit as part of its auto-calibration and thermal stabilization operating functions.

### *3.4. Quantitative Analysis*

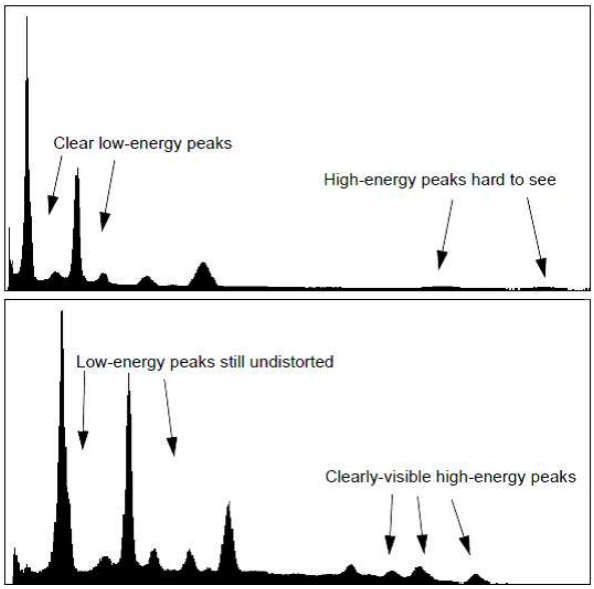


***Figure 7.*** *Spectra of Eu152: top, 1024 channels with linear compression; bottom, 512 channels with Quadratic Conversion Compression (QCC)*

Semiconductor detectors such as high-purity germanium (HPGe) have a linear energy response over its broad detection range from a few keV up to 10MeV. This is not the case with a NaI scintillation detector over its full energy range [14]. This non-linearity interfaced to a linear multi-channel analyzer

(MCA) leads to distorted high-energy peaks. By applying a patented (US patent number: 5,608,222) Quadratic Conversion Compression (QCC) algorithm to the signal processing prior to the MCA the linearization of the energy response effectively un-distorts all the peaks and thereby enhance the speed and accuracy of isotopic identification. Figure 7 demonstrates the effectiveness of applying QCC technology to a commercial NaI scintillator used for nuclear gamma spectroscopy.

Quantitative analysis integrates the total counts in an energy peak attributable to the radionuclide of interest. Baseline background is subtracted to determine the net counts ($N_N$) under the peak area, which can then be cross referenced to the known radioactivity of the age-compensated standard source (as defined in equation 4). The gamma energy emitted by the decay of a radionuclide has an associated branching intensity ratio (i) which must also be factored into the efficiency formula.

$$\varepsilon_A = \frac{N_N}{i.r_0 0.5^{t/\tau_{1/2}}.s} \quad (5)$$

Figure 8 illustrates the determination of the net counts ($N_N$) under a peak area of interest. The shaded trapezoidal area under the peak centroid is the defined background subtracted from the total integrated counts under the peak.

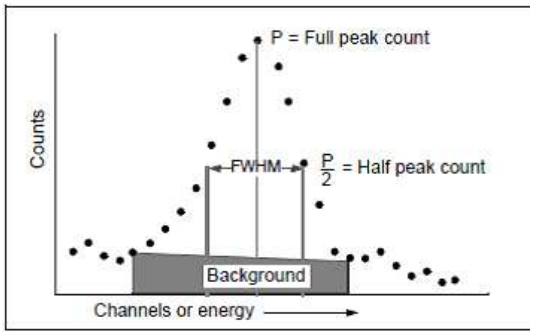


***Figure 8.*** *Determination of peak area*

The reported RIIDEye instrument efficiency calibration was conducted with the age of the sealed NIST standard sources at 216 days. This is longer than the 21 days for full secular equilibrium to be established between Ra226 and its gaseous progeny Rn222 and succeeding short-lived daughter isotopes. Table 4 lists the absolute efficiencies of the calibrated system determined from the energy peaks highlighted in Figures 5 and 6 (excluding 1460keV which belongs to K40).

### *3.5. Field Sampling Tests*

With the instrument fully characterized by calibrating with radium standard sources, field samples were collected and tested with the mobile shielded analyzer that integrates the battery-operated NaI spectrometer and lightweight lead shield. The following site locations were selected and samples placed inside sealed 0.5L beakers.

Seneca Stone Quarry (Lodi, New York): rock samples taken from the Marcellus shale outcrop.

Blacklick Creek (Blacklick, Pennsylvania): sedimentary soil samples and brine water were collected from a wastewater treatment plant (WWTP) pipe discharging treated water directly into the creek. Samples were retrieved at the exhaust point and approximately 0.5km and 1.7km further downstream from the discharge pipe.

Table 5 lists the analyzed results on these varieties of field samples based on the standard 30 minutes measurement time. These field results indicate that a 30 minutes sampling can yield minimum detectable activity (MDA) on the radium decay isotopes of interest for solids above nominally 1pCi/g and for liquids above 1000pCi/L levels. For increased sensitivities the use of a thicker lead shield to reduce background levels or longer measurement times would be required. The continuous discharges from the WWTP into the Blacklick creek over many years have impacted on the accumulated radioactivity in the soil sediment directly at the exhaust point. Although dilution occurs downstream of the discharge pipe, there is still measureable levels of radiological contaminations in the stream sediments approximately 0.5km from source. Previous analysis highlighted in reference [10] in the same Western Pennsylvania locations reported Marcellus shale produced wastewaters has average concentrated radioactivity levels for Ra226 and Ra228 of 3231pCi/L and 452pCi/L, and for treated effluent water of 4pCi/L and 2pCi/L respectively. Chemical analysis also indicates associated high contaminated levels of salinity and toxic metals.

## 4. Conclusion

The application of a mobile analyzer consisting of a shielded NaI gamma spectrometer for rapid screening of hydraulic fracturing wastes has been successfully implemented. Accurate quantifications of contaminated radium isotopes and its associated decay daughters can be achieved by proper efficiency calibrations of the instrument with known standard sources.

***Table 4.*** *Determination of detection efficiencies using standard radium calibrated sources*

| Isotope | Half-Life $\tau_{1/2}$ | Energy (keV) | Intensity (%) | Counts $N_N$ | Efficiency $\varepsilon_A$ |
|---|---|---|---|---|---|
| Ra226 | 1600yr | 186 | 3.6 | 652 | 0.052±0.017 |
| Ra226 (Pb214) | (3.1m) | 242 | 7.4 | 798 | 0.031±0.007 |
| | | 295 | 19.3 | 1343 | 0.020±0.002 |
| | | 352 | 37.6 | 2925 | 0.022±0.001 |
| Ra226 (Bi214) | (19.4m) | 609 | 46.1 | 2289 | 0.014±0.001 |
| Ra228 (Ac228) | (6.15h) | 338 | 11.3 | 1467 | 0.039±0.005 |
| | | 911 | 25.8 | 1565 | 0.018±0.002 |
| Ra228 (Pb212) | (10.64h) | 239 | 43.0 | 8329 | 0.059±0.002 |
| Ra228 (Tl208) | (3.05m) | 583 | 84.0 (35.9) (branching off Bi212) | 2015 | 0.020±0.002 |

***Table 5.*** *Analyzed results of shale produced field samples*

| Sample | Location | Concentration | Isotope | Radioactivity |
|---|---|---|---|---|
| Rock | Seneca outcrop | 776g | Bi214 | 2.3±0.5pCi/g |
| Water | Blacklick pipe | 0.678L | | Nothing above MDA 1000pCi/L |
| Soil | Blacklick pipe | 1078g | Ra226 | 4.7±3.1pCi/g |
| | | | Pb214 | 22.4±0.7pCi/g |
| | | | Bi214 | 27.5±0.3pCi/g |
| | | | Ac228 | 7.6±0.3pCi/g |
| Soil | 0.5km from pipe | 764g | Pb214 | 1.8±0.6pCi/g |
| | | | Bi214 | 2.4±0.3pCi/g |
| | | | Ac228 | 0.6±0.4pCi/g |
| Soil | 1.7km from pipe | 812g | | Nothing above MDA 1pCi/g |

## Acknowledgements

I would like to thank Shale Testing Solutions for supplying the calibrated spectra for my efficiency analysis. To Kolga for providing hardware support to conduct my field tests. To John Stolz (Duquesne University) for providing samples and to Nathaniel Warner (Dartmouth University) for the invitation to participate in the onsite sampling at Blacklick Creek reported in this article.

## References

[1] E. C. Donaldson, W. Alam and N. Begum, Hydraulic fracturing explained: evaluation, implementation, and challenges, Gulf Drilling: Gulf Publishing Company, 2013.

[2] J. Logan, G. Heath, J. Macknick, et al., Natural gas and the transformation of the U.S. energy sector: electricity, The Joint Institute for Strategic Energy Analysis, 2012.

[3] S. G. Osborn, A. Vengosh, N. R. Warner and R. B. Jackson, Methane contamination of drinking water accompanying gas-well drilling and hydraulic fracturing, Proceedings of the National Academy of Sciences, vol. 108, no. 20, 2011, pp. 8172-8176.

[4] G. L. Theodori, A. E. Luloff, F. K. Willits and D. B. Burnett, Hydraulic fracturing and the management, disposal, and reuse of frac flowback waters: views from the public in the Marcellus shale, Energy Research and Social Science, vol. 2, 2014, pp. 66-74.

[5] Radiation protection and the management of radioactive waste in the oil and gas industry, International Atomic Energy Agency, Safety Reports Series No. 34, 2003.

[6] W. Y. Kim, Induced seismicity associated with fluid injection into a deep well in Youngstown, Ohio, Journal of Geophysical Research: Solid Earth, vol. 118, 2013, pp. 1-13.

[7] Chemicals used in hydraulic fracturing, U.S. House of Representatives Committee on Energy and Commerce, 2011.

[8] Study of the potential impacts of hydraulic fracturing on drinking water resources, U.S. Environmental Protection Agency Progress Report 601/R-12/011, 2012.

[9] J. E. Whitten, S. R. Courtemanche, A. R. Jones, R. E. Penrod and D. B. Fogle, Consolidated guidance about materials licenses: program-specific guidance about well logging, tracer, and field flood study licenses, U.S. Nuclear Regulatory Commission, Final Report NUREG-1556, vol. 14, 2000.

[10] N. R. Warner, C. A. Christie, R. B. Jackson and A. Vengosh, Impacts of shale gas wastewater disposal on water quality in western Pennsylvania, Environmental Science and Technology, vol. 47, 2013, pp. 11849-11857.

[11] A. W. Nelson, D. May, A. W. Knight, et al., Matrix complications in the determination of radium levels in hydraulic fracturing flowback water from Marcellus shale, Environmental Science and Technology Letters, vol. 1, 2014, pp. 204-208.

[12] L. Ying and F. O'Connor, TENORM radiological survey of Utica and Marcellus shale, Applied Radiation and Isotopes, vol. 80, 2013, pp. 95-98.

[13] S. N. Kaplanis, Geometric, effective solid angles and intrinsic efficiencies of a 3x3 NaI(Tl) for isotopic and non-isotopic photon emission, International Journal of Applied Radiation and Isotopes, vol. 33, 1982, pp. 127-135.

[14] J. L. Peeples and R. P. Gardner, Monte Carlo simulation of the nonlinear full peak energy response for gamma-ray scintillation detectors, Applied Radiation and Isotopes, vol. 70, 2012, pp. 1058-1062.